Power Electronics and Drives
Volume 11(46), 2026 DOI: 10.2478/pead-2026-0006

Power Electronics and Drives

Optimalisation of Flying Shears Control Structure Using AI Methods

Research Paper

Tadeáš Kmecik*, Matej Hric, Peter Girovský, František Ďurovský

Department of Electrical Engineering and Mechatronics, Faculty of Electrical Engineering and Informatics, Technical University of Košice, Košice, Slovak Republic

Received: 30 December, 2025; Received in the revised form: 11 February, 2026; Accepted: 23 February, 2026

Abstract: Drum-type flying shears represent a technological system used in material processing lines (MPL). During operation, they must withstand an impact shear torque of very short duration with an amplitude comparable to the rated motor torque. The position of the shears is derived from the strip speed, meaning that any change in strip speed is directly reflected in the shears' speed. Therefore, the primary control task is to ensure precise synchronisation between the strip speed and the shears at the moment cutting begins, as well as to minimise the speed drop of the shears during the cutting process. This prevents deformation of the cut strip and deterioration of the dimensional accuracy of the cut sheets. Previous research has shown that conventional control methods supplemented with shear torque compensation can significantly improve speed stability during cutting. Building on these findings, this paper analyses the application of artificial intelligence (AI) elements to optimise the control of flying drum shears. The study compares traditional control approaches with methods based on fuzzy logic and neural networks (NNs), aiming to further improve system dynamics and minimise speed deviations during cutting. The proposed control structures and compensations are verified through simulation, and the results are presented.

Keywords: *artificial intelligence • flying shears • control structure optimisation • neural network • intelligent control*

1. Introduction

Flying drum shears Figure 1 represent a key component of continuous cut-to-length lines, where highly accurate synchronisation of the speed between the driven strip and the rotating knives must be ensured (Ďurovský et al., 2023).

During the cutting process, a sudden increase in shear torque occurs, causing a short-term deceleration of the drive, which may lead to deviations in the cut length and to deformations of the processed material. In addition, accelerated wear of the mechanical components and cutting knives takes place. These impact-related dynamic phenomena are particularly critical at low strip speeds, where the system possesses lower kinetic energy and is therefore more susceptible to speed drops (Magura et al., 2014). A simulation model of such a system was explained in the available literature (Cinquemani and Giberti, 2015).

In industrial practice, conventional P and PI controllers supplemented with feedforward compensation signals are most used for speed control. However, their effectiveness strongly depends on the accurate shape and timing of the shear torque compensation. Changes in material properties, strip thickness, or strip speed may cause improperly tuned compensation to result in increased undershoot and overshoot. In some cases, oscillations of the system may even occur, limiting the robustness and universal applicability of these control approaches. These

* Email: tadeas.kmecik@tuke.sk

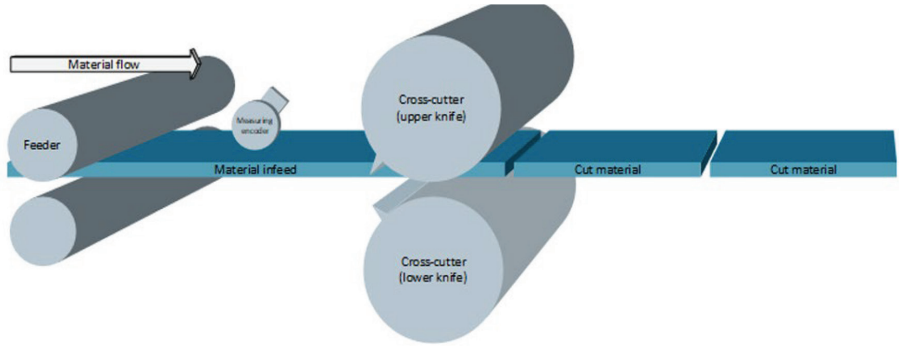

Figure 1. An example of steel sheet cutting on MPL. *Source:* Siemens AG (2025). MPL, material processing lines.

limitations create the need for methods capable of more effectively suppressing impact loads and ensuring a stable dynamic response over the entire operating range (Šlapák et al., 2024).

To further improve the control dynamics of these systems, a drive with direct torque control (DTC) was also analysed, as it enables a fast torque response during cutting (Ng et al., 2017). The influence of vector control of the AC machine on this system was analysed in Solomon and Gaiceanu (2021).

This paper compares classical and advanced shear torque compensation methods to enhance the control dynamics of drum shears. It builds upon previously published work by the authors, addressing the modelling of the shear torque profile, the design of compensation structures and the analysis of servo drive dynamics under various operating conditions (Ďurovský et al., 2023; Šlapák et al., 2024).

In this context, the servo drive dynamics at different strip speeds are analysed, and the limitations of classical P and PI controllers are identified. Furthermore, the effectiveness of conventional, anticipatory and advanced artificial intelligence (AI)-based compensation methods is compared using a unified simulation framework, with particular emphasis on their industrial applicability, adaptability and potential for integration into real control systems.

2. Working Principle of Drum Flying Shears

Flying drum shears consist of a pair of rotating drums equipped with knives that perform a cyclic motion driven by a servo drive. The task of the control system is to ensure precise synchronisation of the circumferential speed of the knives with the speed of the continuously moving strip of the processed material at the instant of cutting, as well as to minimise the speed drop during the cutting process itself (Bi et al., 2020).

The precision of synchronisation directly determines the accuracy of the resulting cut lengths. When the knives penetrate the processed material, the length of the cut format can no longer be influenced. Since the circumferential speed of the knives is derived from the strip speed, it is essential to limit the speed reduction of the knives during cutting. A decrease in knife speed caused by the shear load also leads to a reduction in strip speed, which is immediately reflected as a change in the reference speed of the shears' speed control loop (Bi et al., 2020).

The synchronisation accuracy, together with the dynamic response of the system under the action of the shear torque, has a decisive influence on the cut-length accuracy, cutting quality, the rate of knife wear and the wear of the mechanical components of the entire system (Bi et al., 2020).

During cutting, the drive is subjected to a short duration but significant shear torque, the magnitude of which depends on the material properties, strip thickness and knife geometry. The system's sensitivity to shear loading is strongly influenced by the line speed. At low speeds, the kinetic energy of the mechanical system is low, leading to a higher susceptibility to speed drops, whereas at higher speeds, the increased kinetic energy naturally reduces the system's sensitivity to shear torque.

The control system consists of cascaded drive control loops, comprising a fast current loop that ensures the required torque response and a speed loop responsible for synchronising the knives with the strip motion. To minimise speed drops during cutting, various shear torque compensation strategies are commonly applied in industrial practice.

2.1. Working cycle and movement synchronisation

In the control of flying drum shears, it is necessary to define several reference angular positions and operating zones that ensure proper synchronisation of the knife motion with the moving strip. The positions of the individual reference points (RPs) and zones are illustrated in Figure 2. The fundamental reference for control is the RP, located at the bottom position of the knife trajectory, which serves as the zero angular position for controlling the entire operating cycle.

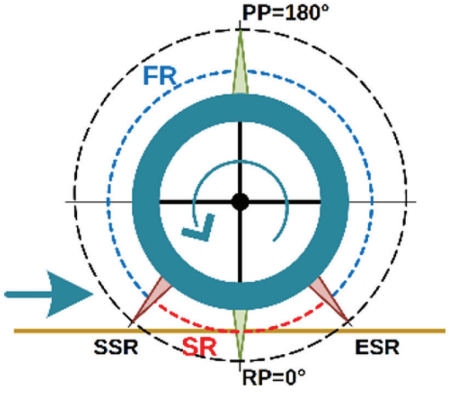

Figure 2. Important areas of rotary shears trajectory. *Source:* Siemens AG (2025). ESR, end of the synchronous range; FR, formatting range; PP, parking position; RP, reference point; SR, synchronous range; SSR, start of the synchronous range.

The operating cycle includes a critical region referred to as the synchronous range (SR), within which the instantaneous circumferential speed of the knives matches the strip speed. Cutting must be performed precisely within this range to minimise relative motion between the knife and the material and to prevent deformations or cut-length errors. The SR is defined by two angular limits: the start of the synchronous range (SSR) and the end of the synchronous range (ESR), which determine the permissible time window for executing the cut.

Outside the SR lies the formatting range (FR), in which the shear speed is intentionally different from the strip speed. The purpose of this zone is to enable dynamic acceleration or deceleration so that the drive reaches synchronous speed at the optimal moment corresponding to the required cut length. For long cut lengths, the shears are often positioned in a parking position (PP), where they remain until the strip reaches the appropriate position for the next cut. The PP is typically set at approximately 180°, corresponding to a mechanically favourable position for both subsequent acceleration and deceleration. For very long cut lengths, the PP may be shifted to extend the available run-up distance and to reduce peak torque demand during acceleration.

These defined RPs and operating zones ensure correct timing of the entire cycle and minimise dynamic loading of the servo drive. They enable precise synchronisation regardless of the current strip speed or cut length and form an essential basis for the design of control strategies and compensation methods discussed in the following sections.

2.2. Energy requirements and the influence of shear torque

In drum flying shears, a single servo drive provides the energy required for both positioning and the cutting process itself. The energy demands of the system are therefore closely linked to the dynamics of the entire operating cycle. The shear torque generated during contact between the knives and the material represents the dominant load, and its magnitude depends on the material thickness, strength and width, the knife geometry, and the cutting speed. (Spišák et al., 2019).

Figure 3 illustrates the ideal motion trajectory of the shears during the operating cycle. To avoid influencing the strip motion during cutting, the projection of the circumferential speed of the knives onto the strip motion direction must be equal to the strip speed. For this reason, at the instant cutting begins, the shears must have a higher circumferential speed, which then decreases smoothly along a cosine-shaped trajectory as the knives pass through the material, reaching the strip speed at the RP, where the speeds of the shears and the strip coincide. As shown in the figure, this speed profile ensures that, under ideal conditions, the shears neither pull nor brake the strip. After

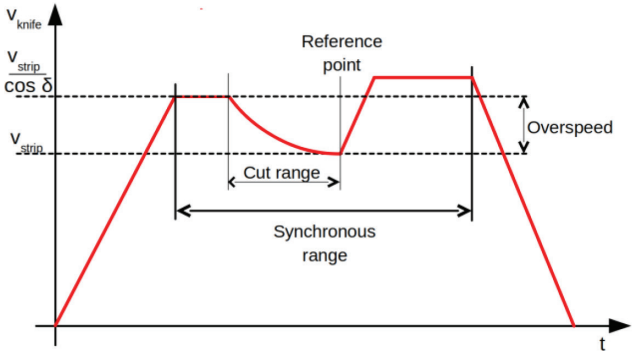

Figure 3. Ideal shears trajectory during the cutting process. *Source:* Ďurovský et al. (2023).

the material has been fully cut, the circumferential speed of the shears must be increased again to allow a smooth transition to the next phase of the operating cycle.

A detailed mechanical and energetic analysis of the cutting process was presented in Šlapák et al. (2024), where transient torque phenomena, dynamic forces and the influence of knife geometry on the energy load of the servo drive were described. In addition, it is reported that knife wear increases the required shear force by approximately 15%–30%.

When cutting thin materials, contact between the knives and the strip occurs close to the reference position, where the tangential speed of the knives is nearly equal to the strip speed. The time during which the knives pass through the strip is very short, and the energy required to cut a thin strip is small; therefore, the kinetic energy of the shears is sufficient to cover this demand. Consequently, the requirements on shear torque compensation in terms of magnitude and timing are not critical. In contrast, when cutting thicker materials or with increased knife overlap, contact between the knives and the material occurs earlier, at a point where the tangential speed of the knives is higher than the strip speed.

The shear torque has an impulsive character with a duration of several milliseconds, and its amplitude may be comparable to the rated motor torque. If this load is not compensated at the correct instant, the shear speed decreases, which slows down the strip and subsequently the shears. Conversely, torque compensation applied too early or with excessive magnitude causes a jerk in the strip motion, which, through positive feedback, results in acceleration of the shears. This phenomenon also has a negative effect on the mechanical components upstream of the shears, particularly the feed rollers and the measuring wheel.

The energy characteristics of the shear torque for a sheet with a thickness of 3 mm, a width of 1,600 mm, and a material tensile strength of 350 MPa at individual angular positions are presented in Table 1, while Table 2 summarises the expected speed drop in the case of free-running operation of the system without control. The rated motor parameters listed in Table 3 provide an indication of the available energy reserve of the servo drive.

Table 1. Shears' position and torque during cut.

Parameters	Shears' angle (°)	Shears' arm (mm)	Torque on motor side	
			(Nm)	(% of T_R)
Beginning of cut	339	34.045	1,872.2	76.14
End of cut	345	24.588	1,352.1	55

Table 2. The shears' angular velocity drop during the cut considering freewheeling shears (i.e. without controllers).

Strip speed (m/min)	Shears' angular velocity			
	Steady state (rad/s)	After cut (rad/s)	Difference (rad/s)	Difference (%)
20	14.74	7.63	7.11	48.34
50	36.847	34.021	2.862	7.77
80	58.938	57.180	1.758	2.98

Table 3. Rotary shears motor parameters.

Parameters	Symbol	Unit	Value
Rated power	P_R	kW	190
Rated voltage	V_R	V	400
Rated speed	n_R	rpm	800
Motor inertia	J_{mot}	kg/m^2	4.2
Rated current	I_R	A	335
Rated frequency	f_R	Hz	27.2
Rated torque	T_R	Nm	2,328
Maximum torque	T_{max}	Nm	4,250
Rated power factor	$\cos(\phi)$	-	0.942
Rated efficiency	η	%	89
Torque control loop time constant	τ_T	ms	2

From the above considerations, it follows that effective control of flying drum shears requires a rapid torque response, accurate shear torque compensation and minimisation of speed drop during cutting, while respecting the drive's energy limits.

2.3. Key challenges in control and the importance of minimising speed drop

The control of drum flying shears is particularly challenging due to the short duration but high shear torque, which has an amplitude comparable to the rated motor torque and lasts only a few milliseconds. This impulse causes a significant speed drop of the shears, especially at low strip speed, where the kinetic energy of the system is insufficient to cover the cutting work. The speed drop has three major consequences:

1. **Degradation of control loop dynamics:** A reduction in shear speed immediately slows down the strip as well, thereby reducing the reference speed. This leads to degraded dynamic performance and may compromise process stability.
2. **Mechanical stress and wear:** Impact-induced load variations in the gearbox, bearings and cutting structure accelerate component wear and increase the energy demand of the cutting process.
3. **Strip from decelerating**: in time, resulting in compressive forces that cause material deformation.

For these reasons, minimising the speed drop during cutting is crucial for maintaining stable system dynamics and extending the service life of mechanical components. The control system must therefore respond at a time scale comparable to the duration of the shear torque and ensure accurate and robust load compensation across a wide range of operating conditions.

3. Control Structure and Compensation Methods

The control structure of the drum shears is shown in Figure 4, which illustrates a cascaded arrangement of the position, speed and torque control loops, supplemented by a trajectory generator and shear torque compensation. The control system utilises references for angular position, speed and dynamic torque generated by the format generator.

The position loop defines the synchronisation phase of the shears with respect to the strip, while the speed loop, employing a PI controller, governs the motion dynamics. The short-duration shear torque acts as an impulsive load applied directly to the torque control loop. To limit the speed drop during cutting, a compensation signal is incorporated into the control structure, augmenting the torque reference during the critical portion of the cycle. This structure serves as a basis for the advanced compensation methods described in the following subsections.

The inner torque control loop is approximated by a first-order transfer function with a dominant time constant $\tau_T = 2$ ms, representing the closed-loop dynamics of the current-controlled drive.

3.1. Conventional PI control with cutting-torque compensation

A previous publication dealing with the analysis of flying drum shear control showed that the best results are achieved by a combination of a speed PI controller tuned according to the criterion of symmetrical optimum, supplemented by dynamic compensation and additional shear torque compensation. This study clearly confirmed that the compensation signal significantly reduces the speed drop during cutting and improves synchronisation between the shears and the material. This approach was therefore adopted as the reference control structure for further optimisation. From the perspective of steady-state accuracy, the speed PI controller must be active before the start of cutting, as it ensures accurate tracking of the smoothly varying speed reference with zero steady-state error, which is crucial for achieving cutting accuracy. However, once cutting begins, the integral component of the PI controller is unable to respond sufficiently fast to the sudden load change caused by the shear torque. This leads to oscillations in shear speed and a reduced ability of the system to accurately follow the speed reference. For this reason, both industrial practice and previous research recommend disabling the integral component of the PI controller during cutting. During the cutting phase, the integrator is unable to react to abrupt load changes, causing overshoots after cutting due to accumulated control error, which prolongs the system settling time. Even after disabling the integrator, the issue of significant speed undershoots caused by the shear torque remains. Therefore, additional shear torque compensation—commonly used in industrial applications—is applied directly to the motor torque reference. The compensation signal typically has a trapezoidal shape, with a higher initial amplitude and a shorter duration than the actual shear torque, to overcome delays in the torque control loop. An example of the load torque, motor torque and compensation signal used in the simulation is shown in Figure 5. This form of control represents the best verified

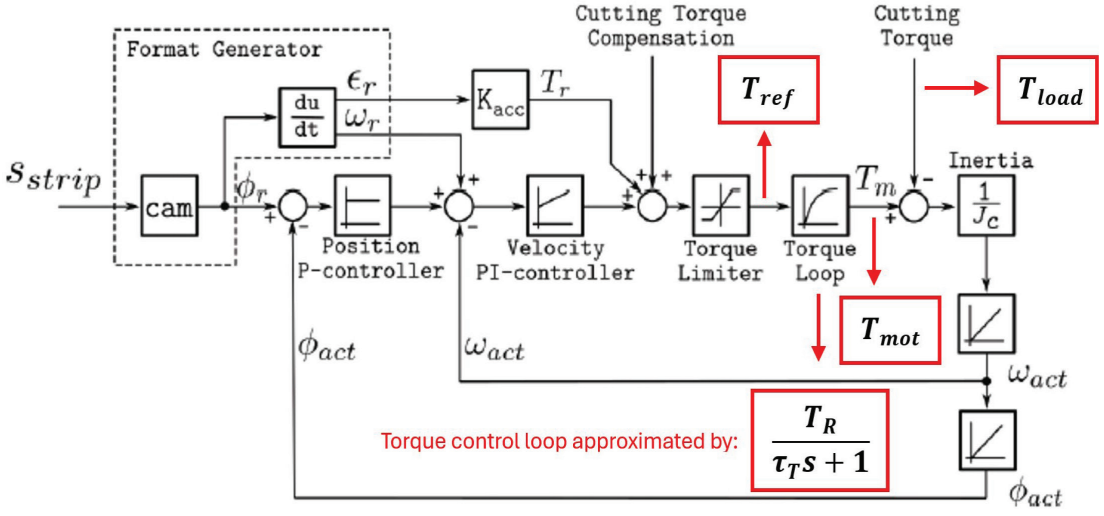

Figure 4. The rotary shears control structure. *Source*: Ďurovský et al. (2023).

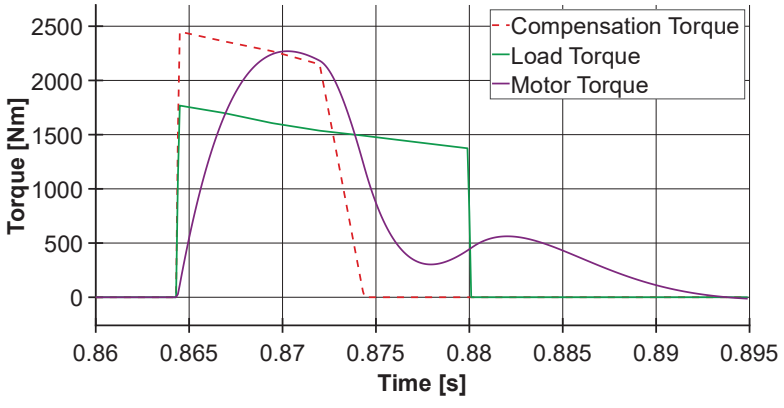

Figure 5. Compensation torque and actual cutting torque during the shearing process.

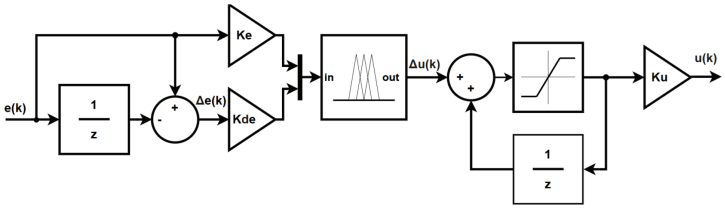

Figure 6. Structure fuzzy controller.

industrial solution to date; however, its performance remains sensitive to changes in operating conditions. These limitations motivate the exploration of further optimisation options in this work. Accordingly, the following sections present two advanced concepts: hybrid control with a fuzzy controller and PI control with optimised compensation using a neural network (NN).

3.2. Hybrid control with PI and fuzzy controller

An extension of conventional PI control is represented by a hybrid approach, in which the PI controller is augmented by a Mamdani-type fuzzy controller. This auxiliary controller is activated exclusively during the cutting process, while the integral component of the PI controller is completely disabled in this mode. The shear torque demonstrates a short-duration behaviour that depends on material properties, strip thickness and the degree of knife wear. Under these conditions, the fuzzy controller represents a suitable means for shear torque compensation and for improving the dynamic response of the system during cutting, without requiring precise identification of the shear torque profile. The fuzzy controller addresses this limitation by directly modifying the torque reference during cutting based on IF–THEN rules. It does not require an accurate mathematical model of the system and naturally handles uncertainties and non-linearities (Lee, 1990a, b). In the proposed hybrid solution, the fuzzy controller utilises the instantaneous speed error $e(k)$ and its change $\Delta e(k)$ to modify the torque reference to minimise the speed drop as much as possible. The structure of the fuzzy controller is shown in Figure 6, where its output $u(k)$ is applied directly to the torque reference. In this way, the hybrid control strategy combines the advantageous properties of PI and fuzzy controllers, enabling improved handling of the dynamic effects of shear torque and achieving a smaller speed drop compared to conventional PI control alone. The output of the fuzzy controller is computed according to the following equation:

$$u(k) = u(k-1) + \Delta u(k) \tag{1}$$

where $u(k)$ represents the compensation signal, $u(k-1)$ denotes the previous value of the compensation signal and $\Delta u(k)$ is the increment of the compensation signal, i.e., the output of the fuzzy system.

3.2.1. Membership functions and fuzzy inference

The fuzzy controller processes two input variables: the speed control error $e(k)$ and its change $\Delta e(k)$. These inputs are normalised using normalisation coefficients K_e and K_{de}. After normalisation, a three-stage Mamdani fuzzy logic procedure is applied: fuzzification, rule-based inference and defuzzification. The membership functions used are shown in Figure 7.

For both inputs and outputs, symmetric triangular membership functions with five linguistic terms were selected: negative medium (NM), negative small (NS), zero (ZE), positive small (PS) and positive medium (PM). This number of linguistic terms represents a compromise between control accuracy and implementation simplicity, which is advantageous for deployment in industrial drive systems with limited computational capacity.

3.2.2. Control rules for fuzzy system

The applied control rules are derived from three meta-principles of fuzzy control. MP1 and MP2 ensure minimal controller intervention in cases of small error or when the error is naturally decreasing, thereby preventing overcompensation. MP3 activates control action in situations where the error does not self-correct and the system requires a fast response. The resulting rule table is presented in Table 4. Each rule defines the instantaneous increment of the control action $\Delta\mu(k)$ based on a combination of $e(k)$ and $\Delta e(k)$. The resulting fuzzy controller is

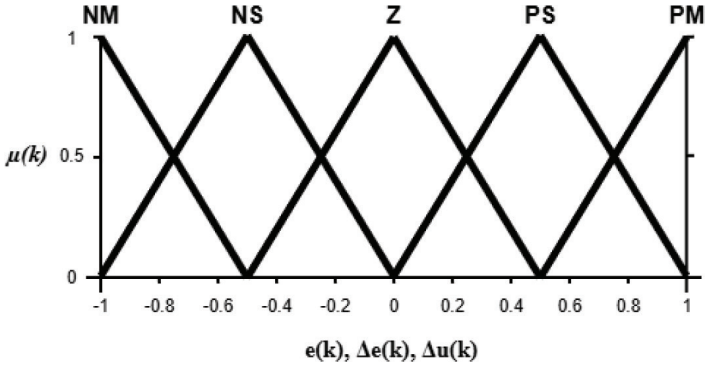

Figure 7. Membership functions of the inputs and output. NM, negative medium; NS, negative small; PM, positive medium; PS, positive small.

Table 4. Fuzzy control rules.

e(k)/Δe(k)	NM	NS	Z	PS	PM
NM	NM	NM	NM	NS	Z
NS	NM	NM	NS	Z	PS
Z	NM	NS	Z	PS	PM
PS	NS	Z	PS	PM	PM
PM	Z	PS	PM	PM	PM

NM, negative medium; NS, negative small; Z, zero; PM, positive medium; PS, positive small.

thus capable of effectively responding to abrupt load changes, supporting more stable system dynamics during cutting. The rule base forms a behavioural matrix of the fuzzy system, in which each increment $\Delta\mu(k)$ depends on the combination of the magnitude of $e(k)$ and the direction of the error change $\Delta e(k)$. This structure enables the fuzzy controller to react efficiently to sudden load variations and thereby enhance the dynamic stability of the system during the cutting process.

3.3. Control with a PI controller and NN–optimised torque compensation

NNs enable effective modelling of non-linear and time-varying systems without the need for an accurate mathematical model, using real data (Bose, 2007; Zhao et al., 2021).

Compared to a simple linear model of the torque control loop, the neural-network-based approach offers the advantage of capturing non-linear effects arising in the complex electromechanical system during the cutting process, thereby enabling more effective optimisation of the compensation signal.

Within this approach, the classical structure of the speed control loop with a PI controller is preserved, while the integral component of the PI controller is disabled during cutting. The control performance is further enhanced by an ideal torque reference profile generated using a NN–based model of the motor torque response. The task of the NN model is to determine, at each computation step, a value of the torque reference that minimises the difference between the motor torque and the load torque and consequently reduces the future speed control error. The model allows multiple candidate torque reference values to be evaluated and selects the one that provides the best dynamic response. In this way, an ideal torque reference profile can be obtained as a function of the drum position, while the NN-based torque loop model is used to evaluate how individual reference values affect the system response in the subsequent step. This enables optimisation of the torque compensation with respect to the known load torque profile during cutting. The result is a hybrid control structure in which the PI controller ensures accurate tracking of the speed reference, while the optimised torque compensation improves the dynamic response of the system during the cutting process.

3.3.1. Predictive NN model of torque loop

For torque compensation optimisation, a feedforward NN model approximating the dynamics of the motor torque response was developed. The model is designed to predict the motor torque value at the next sampling step based

on the current and delayed values of the torque reference T_{ref}, the actual motor torque T_{mot} and the load torque T_{load}. The inclusion of delayed samples enables the internal dynamics of the torque control loop and the system response to control actions to be captured. During model training, the predicted output for time step $k+1$ was obtained by shifting the sampled data forward by one sample. The sampling period was set T = 100 μs. To identify the model, an excitation sequence containing multiple step changes in the torque reference and load torque was generated. The load torque steps were derived from estimated shear torque profiles for different types of materials. The excitation design considered practical constraints of the real drive system, particularly the limits on maximum allowable motor torque, inverter thermal loading and the mechanical strength of the drum shears. At the same time, it was necessary to ensure that the excitation covered the entire operating range of the system, which is essential for creating a generalising model.

The resulting identification dataset provided a sufficiently wide spectrum of operating conditions, enabling the development of a robust, accurate and dynamically consistent predictive NN model of the drive torque response.

The input vector to the NN model has the following form:

$$\mathrm{NN}_{\mathrm{input}}(k) = \begin{bmatrix} T_{\mathrm{ref}}(k) \\ T_{\mathrm{ref}}(k-1) \\ T_{\mathrm{mot}}(k) \\ T_{\mathrm{mot}}(k-1) \\ T_{\mathrm{load}}(k) \\ T_{\mathrm{load}}(k-1) \end{bmatrix} \tag{2}$$

The output of the NN is the predicted motor torque.:

$$\hat{T}_{\mathrm{mot}}(k+1) = f_{NN}\left(\mathrm{NN}_{\mathrm{input}}(k)\right) \tag{3}$$

The output of the NN represents an estimate of the motor torque in the next step, corresponding to the dynamic response of the system to the current torque reference and the acting load torque. The structure designed in this way is particularly well suited for predictive compensation purposes, as it allows the evaluation of also ‘hypothetical’ torque reference values—either during offline optimisation or directly at each step of online computation. As a result, for a given system state, it is possible to quickly and reliably estimate which selected torque reference value will lead to the smallest control error in the subsequent step.

3.3.2. NN architecture and training

The predictive model of the torque control loop was implemented using a feedforward multilayer perceptron (MLP) NN. The task of the network is to predict the motor torque at time step $k+1$, based on the current and delayed values of T_{ref}, T_{mot} a T_{load}. The network was trained using the Levenberg–Marquardt algorithm with normalised inputs and outputs, while the output torque was shifted forward by one sampling step. The dataset contained a wide range of step excitations to cover the entire operating range of the system. The resulting model achieved a low prediction error and good generalisation capability, making it a suitable basis for subsequent optimisation of torque compensation.

3.3.3. Validation of NN model

Validation of the NN model of the torque control loop was performed using a separate test dataset that was not used during model training. (See Table 5). The verification was carried out on multiple dynamic transitions of both the torque reference and the load torque, to capture both steady-state regions and regions with rapid changes. The predicted torque was then compared with the actual measured motor torque.

Evaluation using the mean absolute error (MAE), root mean square error (RMSE), MaxE and the coefficient of determination R^2 see Table 6 confirmed that the NN model very accurately follows the dynamics of the torque loop. Low MAE and RMSE values demonstrate robust average accuracy, while the small maximum absolute error (MaxE)

Table 5. Parameters of NN predictive model.

Parameters	Value/description
Network type	Feedforward NN (MLP)
Output	Prediction of motor torque $\hat{T}_{mot}(k+1)$
Input vector	$\left[T_{ref}(k),\ T_{ref}(k-1),\ T_{mot}(k),\ T_{mot}(k-1),\ T_{load}(k),\ T_{load}(k-1)\right]$
Hidden layers	2
Number of neurons	10–10
Activation functions	Tansig (hidden layers), linear (output layer)
Training algorithms	Levenberg–Marquardt
Input and output normalisation	Range [−1, 1]
Sampling period	$T_s = 100\,\mu$s

MLP, multilayer perceptron; NN, neural network.

Table 6. Performance metrics of the NN torque predictor.

Abbreviation	Full name	Value	Unit
MAE	Mean absolute error	1.7645	Nm
RMSE	Root mean square error	2.3071	Nm
RMSE	Percentage RMSE	0.0991	%
MaxE	Maximum absolute error	5.7528	Nm
R^2	Coefficient of determination	0.9999	-

NN, neural network.

confirms that the model does not exhibit critical deviations even during fast transients. The value $R^2 = 0.9999$ indicates an almost perfect correlation between the predicted and measured torque.

A graphical comparison of the prediction and the actual measurement (see Figure 8) shows very good agreement in amplitude, waveform shape and timing. A detailed view of the prediction error reveals that the deviations are small and do not contain significant systematic or harmonic components.

Based on these results, it can be concluded that the developed NN model is sufficiently accurate, robust and suitable for use in both online and offline optimisation and compensation algorithms.

3.3.4. NN–based optimisation of the torque reference—algorithm and implementation

The computation of the ideal torque reference value represents a key step of the proposed method, in which the classical speed control loop with a PI controller is augmented by predictive NN–based torque compensation. The objective of the algorithm is to determine, at each sampling step, a torque reference value that minimises the control error in the subsequent step. The overall decision-making process is illustrated in Figure 9.

The algorithm utilises the current values $T_{ref}(k)$, $T_{mot}(k)$ and $T_{load}(k)$, as well as their delayed samples. For each candidate value of the tested torque reference, the predicted motor torque at time $k+1$ is computed using the predictive NN model. The optimal torque reference is then selected as the one that shows the minimum value of the error according to the chosen optimisation criterion.

Representative time-domain waveforms of the input signals used for NN training are shown in Figure 10. These waveforms illustrate the response of a PI speed controller with an inner torque loop under constant reference values of the strip speed and various step changes in load torque, which are intended to approximate or simulate the cutting of materials with different geometric dimensions. This data acquisition approach is designed to be applicable not only in simulation environments but also on real drum shears.

3.3.5. Compensation activation—deadband logic

To prevent unnecessary intervention in the control process, compensation is activated only when a defined deadband for both torque and speed is exceeded. The load torque $T_{load}(k)$ depends on the physical cutting process,

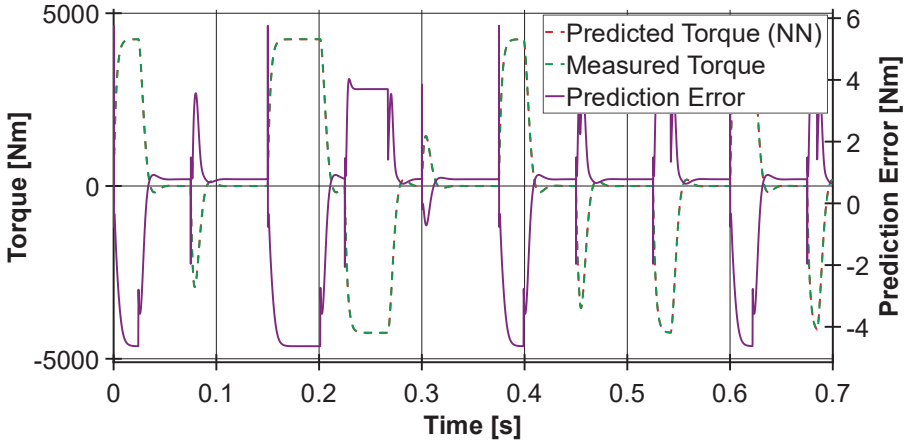

Figure 8. Detailed view of torque prediction error between view of torque prediction error between NN output and measured torque. NN, neural network.

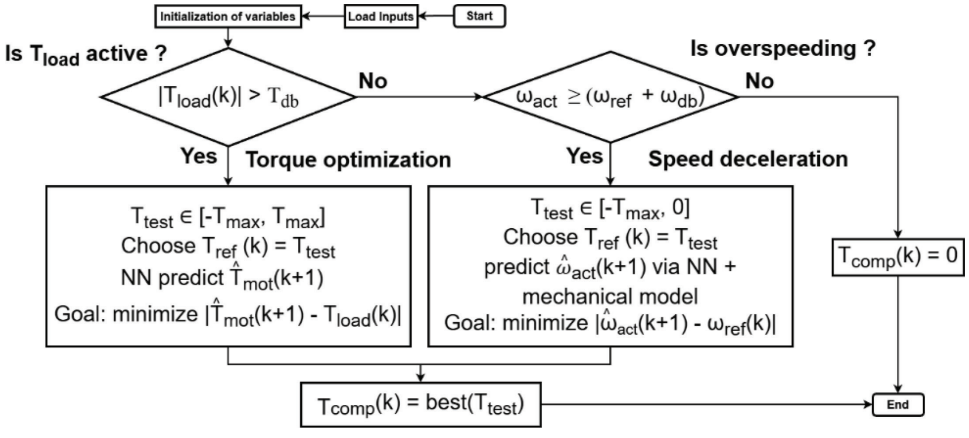

Figure 9. Flowchart of the NN-based torque compensation algorithm. NN, neural network.

and its profile is a function of the drum position. For modelling purposes, experimentally measured shear torque profiles for various materials were used.

- **Torque activation condition**

$$\left|T_{\text{load}}(k)\right| > T_{db} \tag{4}$$

- **Speed activation condition**

$$\omega_{\text{act}}(k) \geq \left(\omega_{\text{ref}}(k) + \omega_{db}\right) \tag{5}$$

These conditions are used in the decision nodes of the flowchart (see Figure 10). If the conditions are not fulfilled, the compensation is disabled $T_{\text{comp}}(k) = 0$.

3.3.6. Prediction of torque and speed

The predicted motor torque at time step $k+1$ is obtained using the NN model:

$$\hat{T}_{\text{mot}}(k+1) = f_{\text{NN}}(u(k)) \tag{6}$$

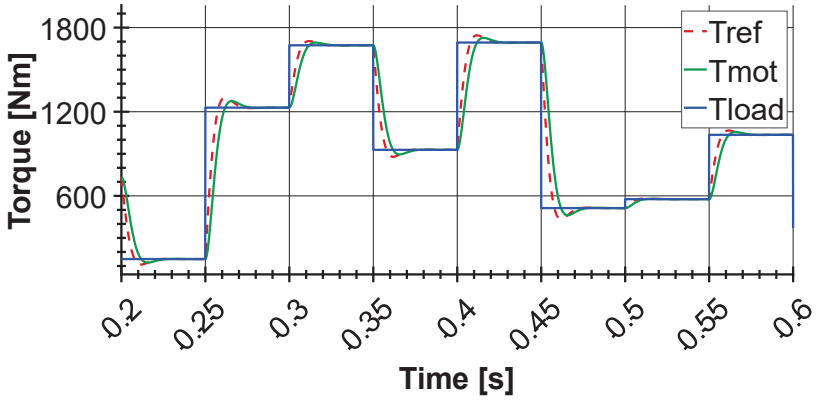

Figure 10. Input signals used for NN training in the time domain. NN, neural network.

Where $u(k)$ = [$T_{ref}(k)$, $T_{ref}(k-1)$, $T_{mot}(k)$, $T_{mot}(k-1)$, $T_{load}(k)$, $T_{load}(k-1)$]. The speed prediction is computed by combining the predicted torque with an analytical mechanical model:

$$\hat{\omega}_{act}(k+1) = \omega_{act}(k) + \frac{T_s}{J}\left(\hat{T}_{mot}(k+1) - T_{load}(k)\right) \tag{7}$$

3.3.7. Optimalisation modes (see Figure 9)

Algorithm works in two modes:

(a) Torque optimalisation (during cutting)

$$T_{test} \in \left[-T_{max},\ T_{max}\right] \tag{8}$$

minimisation criterion:

$$\min\left|\hat{T}_{mot}(k+1) - T_{load}(k)\right| \tag{9}$$

(b) Speed braking mode (After load relief)

$$T_{test} \in \left[-T_{max}, 0\right] \tag{10}$$

minimisation criterion:

$$\min\left|\hat{\omega}_{act}(k+1) - \omega_{ref}(k)\right| \tag{11}$$

Choosing the optimal value:

$$T_{comp(k)} = \text{argmin}_{\{T_{test}\}}\{\text{criterion}\} \tag{12}$$

3.3.8. Online and offline mode of calculation for the optimal reference

a) Online mode

- The ideal torque reference is computed at each control step.
- The advantage of this approach is its adaptation to real system variations and the current state of the drive.
- The compensation operates directly with the actual values of $T_{mot}(k)$ and $T_{load}(k)$.

b) Offline mode

- The known profile of $T_{load}(k)$ as a function of the drum position is used as a deterministic input.
- The NN model predicts $T_{mot}(k+1)$ for the tested values of $T_{ref}(k)$. For the next step, the predicted torque $\hat{T}_{mot}(k+1)$ from the previous step is used as an input to the NN.
- The network does not require measurement of real values at each step.
- The prediction process is performed recursively based solely on the NN model and the known $T_{load}(k)$.

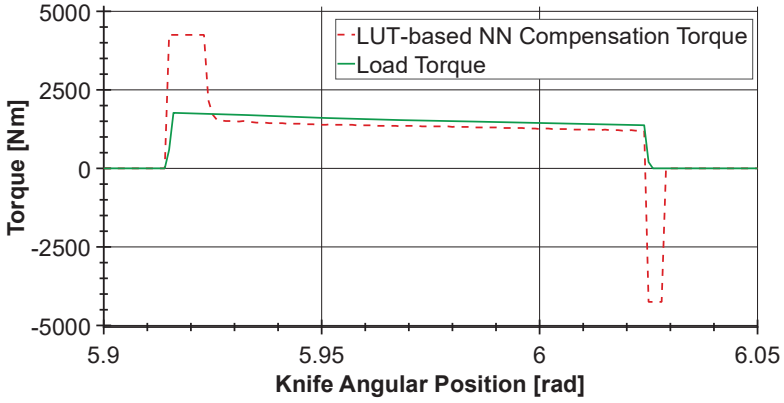

Figure 11. Comparison of the 1D lookup-table-based compensation torque and the load torque. LUT, lookup table; NN, neural network.

- The result is an ideal torque reference profile for the entire cutting cycle, which is subsequently stored in a lookup table (LUT).

The key advantage of the offline mode lies in the fact that the algorithm can autonomously simulate the system response using the NN–based prediction, thereby enabling the generation of optimal torque reference values without the need for real-time measurements at each step.

The compensation torque is stored in a LUT indexed by the angular position of the drum Figure 11. The activation of the compensation signal is controlled by the angular position of the cutting drum. The exact cutting instant depends on the geometric properties of the processed material. For thicker or wider material, the cutting instant occurs earlier.

4. Simulation Analysis of the Proposed Concepts

This section presents and analyses the influence of the controller type and the shape of the compensation signal on the motor speed and torque responses during the cutting process. The objective is to demonstrate how different control structures affect the dynamic response of the drive under impact loading, with particular emphasis on speed reference tracking accuracy, the absolute and relative speed drop during cutting, and the motor torque behaviour during subsequent stabilisation.

Figures 12a–f illustrate the speed and torque responses for the individual tested control and compensation approaches under identical cutting conditions. Figure 12a shows the reference response obtained using a basic P controller, while Figure 12b presents control using a PI controller. In both cases, shear torque compensation is disabled. Figure 12c depicts P control supplemented with a separate compensation signal, and Figure 12d shows P control extended by anticipatory compensation applied before the expected shear load. The time advance of the compensation relative to the cutting instant was determined using a trial-and-error method and optimised for a strip speed of 40 m/min. Figure 12e presents P control augmented with a fuzzy controller, and finally Figure 12f illustrates the control structure in which the compensating torque is generated by a NN model stored in the form of a LUT.

The presented responses form the basis for the subsequent comparison of the dynamic properties of the individual methods.

The simulation parameters are based on a real drum shear system described in previous publications on which this work is built. An AC drive is considered in simulations. For this reason, and based on the authors' practical experience, the time constant of the torque control loop was set to 5 ms in the simulations (Ďurovský et al., 2023; Šlapák et al., 2024).

In the practical operation of this type of equipment, operation in the field-weakening region is not considered. Therefore, the control loops of the torque-producing and flux-producing current components can be modelled as first-order systems. The shear torque compensation is added to the dynamic compensation (Ďurovský et al., 2023; Šlapák et al., 2024).

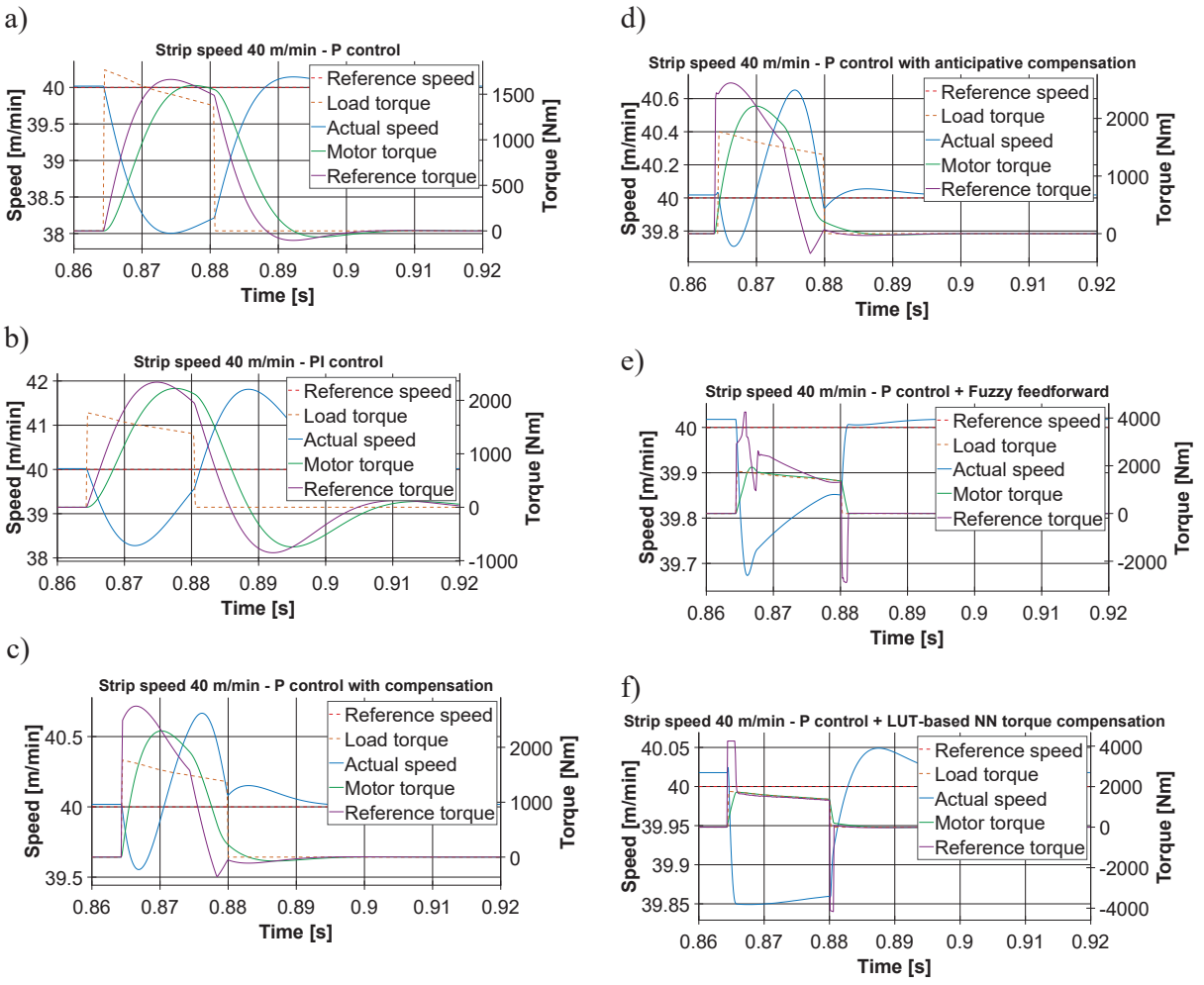

Figure 12. Simulation results of cutting 3 mm thick and 1,600 mm wide strip at 40 m/min. (a) P-type controller without compensation, (b) PI-type controller without compensation, (c) P-type controller with compensation, (d) P-type controller with anticipative compensation, (e) P-type controller with Fuzzy feedforward, (f) P-type controller NN-based LUT compensation. LUT, lookup table; NN, neural network.

with anticipatory compensation proving to be particularly effective. It should be emphasised that the anticipation time was tuned specifically for this speed range. The advanced methods again provide the best performance.

At the highest speed of 80 m/min, the drive possesses the greatest kinetic energy, which naturally suppresses the impact of step-like disturbances and results in the smallest differences among the controllers. Although P and PI controllers without compensation achieve better results than at lower speeds, their settling times remain longer compared to the advanced methods. Compensation strategies, both simple and anticipatory, reduce the speed drop to below 0.6%, with the NN-optimised compensation achieving the lowest undershoot. The combination of a P controller and a fuzzy controller provides the shortest settling time in this speed range.

The comprehensive comparison shows that classical P and PI controllers without compensation generate the largest speed drops (5%–11%) and the longest settling times. Compensation methods significantly improve the dynamic response; however, the anticipatory approach may lead to system oscillations and increased speed overshoot if the timing or signal shape is not optimal. Among the advanced methods, the P controller combined with a fuzzy controller demonstrates high dynamic performance across all speeds, comparable to the NN-optimised compensation. In contrast, the NN-optimised compensation achieves the lowest speed drop and the most stable response over the entire operating range, making it the most effective solution among the analysed approaches.

Table 7. Summary of dynamic performance metrics for all tested control structures and compensation strategies at different strip speeds.

Strip speed [m/min]	Control structure	Compensation	Speed drop [%]	Absolutely speed drop [m/min]	Speed overshoot [%]	Settling time [ms]
20	P	No	10.71	2.144	0.115	54.2
	PI	No	9.12	1.824	1.534	82.3
	P	Yes	4.74	0.948	4.38	50.1
	P	Anticipative	5.71	1.143	4.21	50.7
	P + fuzzy	No	1.66	0.332	0	34.7
	P	NN compensation	1.07	0.214	0.06	35.7
40	P	No	5.03	2.014	0.32	34.5
	PI	No	4.35	1.740	4.48	53.1
	P	Yes	1.16	0.464	1.62	25.5
	P	Anticipative	0.78	0.311	1.58	16.6
	P + fuzzy	No	0.86	0.344	0	16.2
	P	NN compensation	0.55	0.222	0.02	19.4
80	P	No	2.28	1.825	0.13	23.5
	PI	No	2.03	1.621	1.47	44.2
	P	Yes	0.56	0.448	0.52	19.8
	P	Anticipative	0.47	0.377	0.45	19.5
	P + fuzzy	No	0.43	0.344	0	8.3
	P	NN compensation	0.28	0.226	0.01	10

NN, neural network; PI, proportional–integral.

Simulations were performed for three strip speed values. First, a speed of 20 m/min was simulated, followed by 40 m/min, for which time responses of the analysed variables were also plotted. In addition, the maximum operating speed of 80 m/min was simulated. The values obtained from the simulations are clearly compared in Table 7.

The speed PI controller of the shears was designed according to the symmetrical optimum criterion. The P controller, as well as the normalisation and denormalisation constants of the fuzzy controller, were tuned using a trial-and-error approach, in accordance with common practice. The tuning objective was to minimise the speed drop while maintaining robustness of the control against possible measurement and system noise.

4.1. Simulation results

Simulations were performed for three strip speed values—20 m/min, 40 m/min and 80 m/min. For each speed, various control structures and torque compensation strategies were analysed. Control performance was evaluated using four measured indicators: percentage speed undershoots, absolute speed undershoot, percentage speed overshoot and settling time. The summarised numerical results are presented in Figure 7, followed by an interpretation of the observed outcomes.

At the low speed of 20 m/min, the system is most sensitive to dynamic disturbances, as the low kinetic energy of the strip significantly amplifies the influence of the shear torque on the drive speed error. In this operating regime, the basic P and PI controllers without compensation exhibit the largest speed drop as well as the longest settling times.

The introduction of compensation significantly reduces the speed undershoot; however, an anomaly can also be observed in which a non-optimal compensation shape and anticipation timing lead to a pronounced increase in speed overshoot. The best results at low speeds are achieved using a P controller combined with a fuzzy controller and the NN-optimised compensation. These methods minimise the speed undershoot, practically eliminate overshoot and ensure the fastest dynamic response.

At a strip speed of 40 m/min, the system dynamics are naturally stabilised by increased kinetic energy, which reduces the differences between the individual controllers. Nevertheless, P and PI controllers without compensation continue to exhibit significant speed undershoot and overshoot, with the PI controller producing the largest deviations. Compensation methods in this range substantially shorten the settling time and reduce the speed drop,

4.2. Discussion and evaluation of the simulation results

The simulation results presented in Table 7 confirm significant differences in the dynamic behaviour of the individual control structures. Basic P and PI controllers without compensation exhibit the largest speed undershoots and the longest settling times, and they are most sensitive to step disturbances at low strip speeds. Therefore, the use of these basic structures in the low-speed operating range is not recommended.

Introducing compensation to the P controller significantly improves the dynamic response of the system, with the anticipatory version achieving better results particularly at medium and higher speeds. However, in the low-speed range, anticipatory compensation exhibits increased speed overshoot, which is a consequence of non-optimised signal shape and timing for this operating regime. To achieve optimal performance, both conventional and anticipatory compensation require a certain degree of adaptivity, especially at low speeds, where inaccurate timing or an unsuitable compensation signal shape may lead to undesirable oscillations and degraded system stability. A significant drawback of this method is the time-consuming tuning process and the search for the optimal compensation shape and anticipation timing, as both parameters depend on the properties of the cut material as well as on the current strip speed.

Fuzzy control and NN–based compensation achieve the best results across all tested speeds. Both methods minimise the speed drop while ensuring high control dynamics without pronounced overshoot. The fuzzy method provides the shortest settling time, and an additional advantage is its relatively simple tuning procedure. On the other hand, its integration into industrial control personal computers (PCs) can be more demanding, which may limit its practical deployment.

NN–optimised compensation exhibits the most consistent response and the lowest speed drop over the entire speed range. Although this approach requires identification of the torque response of the real system, it offers a significant advantage in that the optimal compensation signal shape can be obtained offline for a specific shear torque profile. The optimised compensation profile can then be easily implemented in a programmable logic controller (PLC) using a LUT, even in multiple variants for different materials and operating conditions. An additional advantage is that the NN is trained on data from the real system, inherently capturing parasitic non-linearities.

Overall, it can be concluded that the application of advanced compensation methods significantly enhances the stability and dynamic performance of drum shear control. Compared to classical P and Proportional–Integral (PI) controllers, both fuzzy and NN–based methods provide several-fold improvement in speed tracking under step disturbances, making them particularly suitable for modern high-speed production lines where precise drive synchronisation is critical.

5. Conclusion

This paper analysed the control of flying drum shears with a focus on minimising the speed drop caused by impulsive shear torque. Based on a developed simulation model, conventional control structures were compared with advanced compensation methods, including fuzzy control and NN–optimised torque compensation.

The simulation results confirmed that basic P and PI controllers without compensation are unable to ensure sufficient dynamic performance at low strip speeds and exhibit significant speed drops. The introduction of shear torque compensation substantially improves system behaviour; however, classical and anticipatory compensation approaches remain sensitive to changes in operating conditions and require demanding tuning procedures.

Advanced methods based on fuzzy control and NNs achieved the best results across the entire tested speed range. Fuzzy control provided a very fast dynamic response and complete elimination of speed overshoot, while the NN-optimised compensation achieved the lowest speed drop and the most stable system behaviour.

A significant advantage of the NN–based approach is the possibility of offline optimisation of the compensation signal and its straightforward implementation in an industrial control system in the form of a LUT. Moreover, the influence of knife wear on the optimal compensation profile can be incorporated into the model, allowing changes identified in the real system to be directly reflected in the control strategy.

Based on the obtained results, it can be concluded that the use of AI elements represents an effective means for further enhancing the dynamic performance of flying drum shear control. The proposed methods provide a solid foundation for future experimental validation and industrial deployment in modern high-speed cut-to-length production lines.

Acknowledgements

This work was supported by the Scientific Grant Agency of the Ministry of Education of the Slovak Republic under project APVV-23-0521 and by the European Union's NextGenerationEU programme through the Recovery and Resilience Plan for Slovakia under project No. 09I05-03-V02-00018.

References

Bi, J., Fan, W., Huang, H. and Liu, B. (2020). Reliability Design of an Electronic cam Curve for Flying Shear Machine in Short Materials Cutting. *Journal of Shanghai Jiaotong University (Science)*, 25, pp. 246–252. doi: 10.1007/s12204-019-2106-2

Bose, B. K. (2007). Neural Network Applications in Power Electronics and Motor Drives—an Introduction and Perspective. *IEEE Transactions on Industrial Electronics*, 54(1), pp. 14–33. doi: 10.1109/TIE.2006.888683

Cinquemani, S. and Giberti, H. (2015). An innovative tool for simulation and control of a flying-cutting machine. In: M. Mains, ed., Topics in Modal Analysis, Volume 10. *Conference Proceedings of the Society for Experimental Mechanics Series*. pp. 227–235. Cham: Springer, doi.org/10.1007/978-3 319-15251-6_21.

Ďurovský, F., Šlapák, V., Smoleň, P., Kyslan, K. and Spišák, E. (2023). Rotary shears control in material processing lines. In: *Proceedings of the 2023 International Conference on Electrical Drives and Power Electronics (EDPE)*, High Tatras, Slovakia, pp. 1–9. doi:10.1109/EDPE58625.2023.10274059.

Lee, C. C. (1990a). Fuzzy Logic in Control Systems: Fuzzy Logic Controller – Part I. *IEEE Transactions on Systems*, 20(2), pp. 404–418. doi: 10.1109/21.52551

Lee, C. C. (1990b). Fuzzy Logic in Control Systems: Fuzzy Logic Controller – Part II. *IEEE Transactions on Systems, Man, and Cybernetics*, 20(2), pp. 419–435. doi: 10.1109/21.52552

Magura, D., Fedák, V. and Kyslan, K. (2014). Modeling and Analysis of Multi-Motor Drive Properties in a Web Processing Continuous Line. *Procedia Engineering*, 96, pp. 281–288. doi: 10.1016/j.proeng.2014.12.155

Ng, G., Deleanu, S., Prévost, J.-P. and Carpenter, D. (2017). Improving the operation of a flying dividing shear by using Direct Torque Control. In: *2017 International Conference on Modern Power Systems (MPS)*, Cluj-Napoca, Romania, pp. 1–8. doi: 10.1109/MPS.2017.7974419.

Siemens AG (2025). *SIMATIC Rotary Knife: Standard Application Manual*. Version 1.5.0, Entry ID: 109757260. Siemens Industry Online Support, Siemens AG.

Šlapák, V., Ďurovský, F., Kyslan, K. and Smoleň, P. (2024). Shearing Work Analysis and Control Design of Rotary Shears in Material Processing Lines. *Power Electronics and Drives*, 9(44), pp. 482–501. doi: 10.2478/pead-2024-0030

Solomon, M. G. and Gaiceanu, M. (2021). The optimization of the dynamic regime of the asynchronous vectorial AC motor in flying shear. In: *7th International Symposium on Electrical and Electronics Engineering (ISEEE)*, Galati, Romania, 1–6. doi: 10.1109/ ISEEE53383.2021.9628488.

Spišák, E., Slota, J., Majerníková, J. and Dulebová, Ľ. (2019). *Production Technologies – Forming, Cutting, Injection Molding*, 1st ed. Košice: Technical University of Košice, ISBN: 978-8-0553-3383-3380.

Zhao, S., Blaabjerg, F. and Wang, H. (2021). An Overview of Artificial Intelligence Applications for Power Electronics. *IEEE Transactions on Power Electronics*, 36(4), pp. 4633–4659. doi: 10.1109/TPEL.2020.3024914